DESIGN STUDY OF AN ACTIVE GURNEY FLAP SYSTEM FOR HELICOPTER ROTOR BLADES

Y. Lemmens, H. Erdelyi, T. Olbrechts
LMS International
Yves.lemmens@lmsintl.com

Keywords: *Co-simulation, Active Gurney Flap, Helicopter rotor blade*

Abstract

A preliminary design of an integrated active Gurney flap system for helicopter rotor blades has been investigated. It is composed of 3 sub-systems, namely the blade with flaps mechanism, a piezoelectric stack actuation system and a controller. The analysis of the integrated system is based on co-simulation between three separate tools that models each sub-system.

1 Introduction

The objective of this paper is to present a conceptual design study for an active flow control system that can be embedded in a blade of a helicopter rotor. This research reports on the work that has been undertaken in the framework of the European research project JTI Clean Sky - Green Rotorcraft [1]. One of the tasks of this project is to investigate novel systems for smart helicopter rotor blades. A technology review by the partners resulted in the selection of an active Gurney flap (AGF) system to be investigated for controlling the airflow conditions around the blade of a rotor. Furthermore, piezo-electric actuators have been suggested and studied in the project technology review [7]. Therefore, this design study will focus on these types of actuators.

The concept of the AGF is a flap that is deployed normal to the blade surface and is as close as possible to the trailing edge of blade during the retreating phase of the blade in order to increase the lift [11] [12]. However, the flap should be stowed to minimize the drag during the forward moving phase of the blade. As a result, the flap will be deployed and retracted very rapidly during the rotation of the helicopter blade which will result in high dynamic behaviour.

2 Three-Level Co-simulation methodology

Modelling the complete active Gurney flap system integrated in a helicopter blade requires the development of three models representing three different subsystems:

- Mechanical subsystem composed of the blade and gurney flap mechanism
- Actuation subsystem composed of piezo-electric stack actuator and its electrical circuit
- Control system which controls the deployment of the AGFs

In order to simulate the complete active Gurney flap system, the above mentioned models of the different subsystems have to be merged in a co-simulation environment. In the present case the mechanical subsystem of the actuation mechanism of the AGF integrated in a helicopter blade was modelled using multi-body simulation [3] software LMS Virtual.Lab Motion [6]. The piezo-electric stack actuator with its electrical circuit was modelled in LMS Imagine.Lab AMESim [5]. To be able to control the deployment of the AGF, a basic controller was developed using Matlab/Simulink. To be able to link the three different models developed in three different software packages a co-simulation architecture was adopted as presented in Fig 1. According to this architecture, the mechanical model of the actuation mechanism was integrated in the piezo-electric actuation system. Subsequently,

the actuation system model was linked to the controller model.

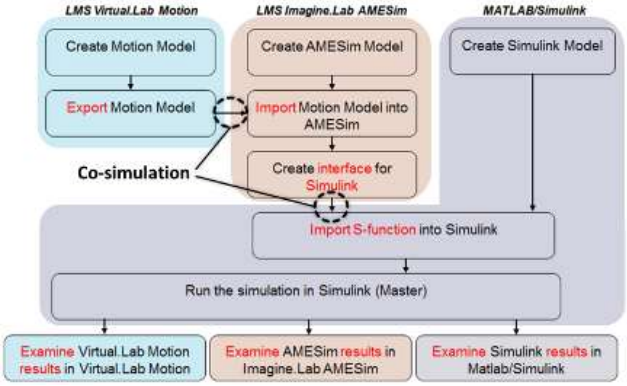

Fig 1. 3-Level co-simulation architecture

In the adopted co-simulation architecture Matlab/Simulink was the master, meaning that the simulation was started from Simulink which was also in charge to link the software packages and set up the communication [2]. Consequently, the communication time interval when the different models in the different software packages exchange their information was also handled by Simulink.

This co-simulation architecture has the benefit that different components can be plugged together to assess different designs without the need to change the other models, for example different actuators can be plugged into the actuation model and run the co-simulation, without the need to change the mechanical model in Motion or the controller in Simulink. Consequently the input and output signals were the following:

- OUTPUT to LMS Virtual.Lab Motion: Force, which is driving the mechanism in order to be able to deploy the AGF
- INPUT from LMS Virtual.Lab Motion: Position and velocity of the connection point to the mechanism
- OUTPUT to Matlab Simulink: actual position of the mechanism
- INPUT from Matlab Simulink: Voltage level for actuation system

The controller modelled in Simulink, takes as input the displacement of the connection point of the piezo electric actuator to the actuation mechanism measured in mechanical system and based on this, calculates the control voltage of the piezo actuator's electrical circuit. Consequently it controls the stroke of the piezo electric actuator and implicitly the deployment of the AGF.

3 Multi-body rotor model

To investigate a design and simulation methodology for an active gurney flap that is embedded in a helicopter main rotor blade, a multi-body model of a blade was needed. A model of a rigid blade was created based on the baseline blade definition for the Clean Sky GRC1.1 working package by AgustaWestland in [8]. This is a fully articulated blade with the lead-lag, flap and pitch hinges at the same location. Therefore, this hinge was modelled with three coincident revolute joints. For the lead-lag damper, a translational spring-damper-actuator was associated with the specified non-linear damping curve. Also a quarter of the rotating swash plate was modelled and connected to the blade with a spring with the prescribed push rod stiffness.

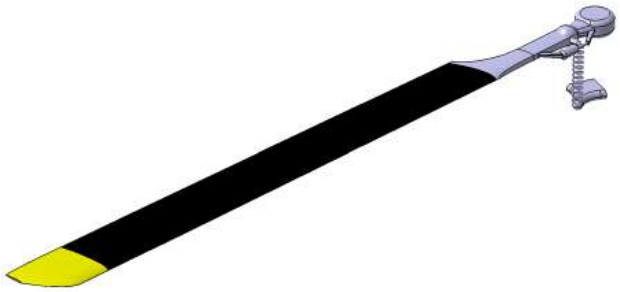

Fig 2. LMS Virtual.Lab Motion blade model

In order to validate the dynamic behaviour of the rotor model, a modal analysis can be performed to assess its natural frequencies of the fundamental lead-lag and flap modes at different rotational regimes. This can be compared with the data provided on reference blade in the Clean Sky GRC project. To determine the natural frequencies of the blades, a linearization can be performed at every time step during the multi-body simulation. Consequently, at every time step, the eigenvalues and eigenvectors of the blade are obtained. Once the blade is in steady-state, the eigenvalues should remain constant. As a result, a Campbell diagram of the fundamental lead-lag

and flap mode can be produced as shown in the figure below (Fig 3.). This corresponds closely to the reference data [11].

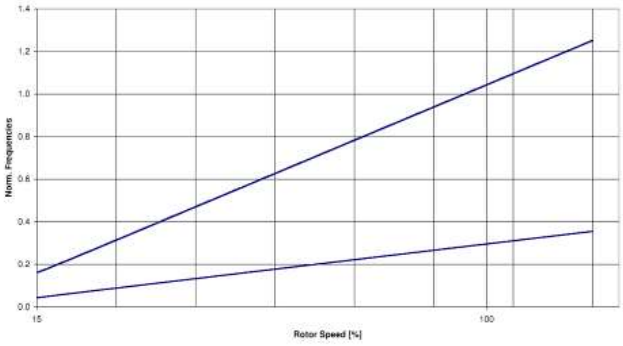

Fig 3. Campbell diagram of fundamental lead-lag and flap modes

4 Aerodynamic load

As presented in Fig 4, the first step in defining the aerodynamic loads on the AGF in the multi-body simulation model was to determine from the CFD results of NLR the highest load and the related parameters. Since the aerodynamic force will be modelled as concentrated vector force rather than a distributed force, the next step was to calculate the resultant aerodynamic force on an AGF of the width of ΔX. Finally, considering the characteristics of the piezo-electric stack actuators the transmission ratio of the actuation mechanism and the corresponding optimal AGF width could be calculated.

For the aerodynamic force calculation the "worst case scenario" was considered. Due to the fact that the tangential component is 1e-5 times the normal component, the tangential forces are neglected. Also the pitching moment will be neglected. The aerodynamic force is computed with the following equation:

$$F_{aero} = \frac{1}{2}\rho_{air} L_{GF} (\varpi R - V_{heli})^2 c_n \qquad (1)$$

The helicopter speed V_{heli} is considered 0 as this will result in the highest aerodynamic forces on the retreating blade.

Considering that the aerodynamic force is a parabolic function and the resultant force is the area below the parabolic function of the distributed aerodynamic force, the resultant aerodynamic force over a Gurney flap span of ΔX= R1-R0 (along the blade radius from R0 to R1) is computed with the following equation:

$$F_{aerores} = \frac{1}{3}\left(\frac{1}{2}\rho_{air} L_{GF} \varpi^2 c_n\right)\left(R_1^{\,3} - R_0^{\,3}\right) \qquad (2)$$

Subsequently, the transmission ratio of a lever mechanism for a give aerodynamic is computed with the following equation:

$$TR_{Max/Min} = \left[1 \pm \sqrt{1 - \frac{4F_{aerores} D_{max} \Delta X}{F_{block} D_{free}}}\right] \Big/ \left[\frac{2F_{aerores} \Delta X}{F_{block}}\right] \qquad (3)$$

As discussed in a previous publication [4], this equation computes the maximum and minimum transmission ratios for a given gurney flap width ΔX considering the resultant force also for the same gurney flap width ΔX.

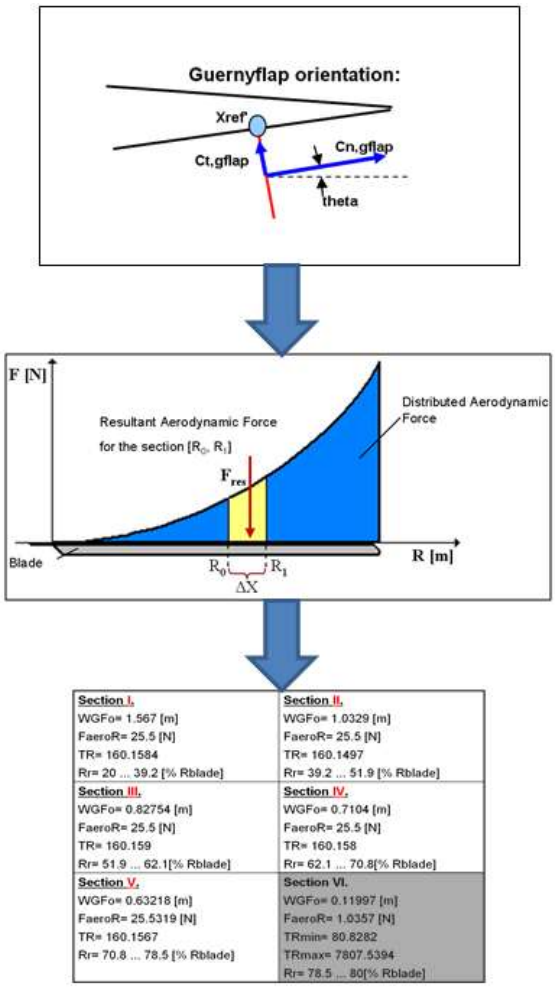

Fig 4. Aerodynamic load calculation method

5 AGF operating condition

The Dutch national aerospace laboratory (NLR) defined the optimum Gurney-flap ranges for different helicopter speeds and loads as presented in the circular plot in Fig 5. As an initial value, the Gurney flaps were considered to deploy and retract over 10deg azimuth angle.

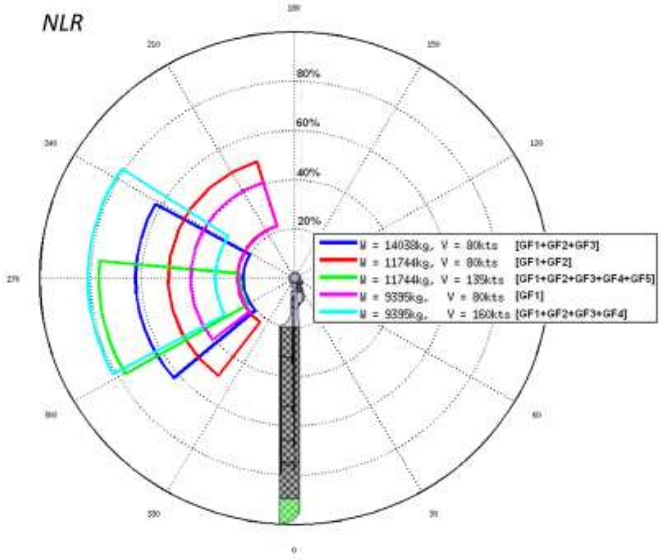

Fig 5. Optimum gurney-flap ranges for different helicopter speeds and loads (courtesy of NLR)

According to this plot, 5 cases can be defined for which AGFs need to be deployed on different blade spans. For example in case of the 4th operating condition the gurney flaps need to cover from 20% to 40% of the blade span corresponding to a AGF width of 1.63 [m]. Subsequently, a piezo-electric stack actuator had to be selected. The optimal actuator delivers the largest power for the least weight. The review and selection of the actuator has been discussed in previous publications [9] [10]. Taken into account the above discussed aerodynamic force calculation, the required number of actuators can be computed for the maximum length as determined by the NLR, i.e. from approximate 20% till 80% of the blade length. This results in the need for 6 of the selected actuators to be able to deploy the gurney flaps of the maximum length. For each flap, the optimal length and transmission ratio to its actuator is obtained. However, the sixth AGF width is very short and consequently it would be ineffective to add the extra actuation mechanism and its piezo-electric stack actuator to deploy it. Therefore this AGF was not considered further and as such 5 AGFs were used in the conceptual design, hence reducing slightly the range of gurney flaps along the blade.

Consequently, for each actuator a corresponding AGF length can be calculated. As the aerodynamic force varies along the blade span, the AGF length will also vary accordingly. Table 1 presents for the different 5 operating conditions, the AGF combinations that match the required blade spans. The Error column in the table shows the difference in percentage of the required blade span with the available AGFs calculated width. In this column a negative value means that the blade span covered by the AGFs is less than required. A positive value means that the AGFs cover more of the span than required. It can be observed that the AGFs cover almost perfectly the different blade spans corresponding to the different operating conditions with the highest error being only -4.4% in case of the second operating condition.

OC	AGFs used	Error (%)
I	1+2+3	1.70
II	1+2	-4.40
III	1+2+3+4+5	-2.28
IV	1	-0.48
V	1+2+3+4	0.48

Table 1: Helicopter operating conditions

The information in the table above was used in the controller design in Simulink. In this controller the user can select one of the different conditions and accordingly the required AGFs will be deployed and retracted with the corresponding azimuth angles.

6 Conceptual design study

Based on the design methodology that has be developed and published before [4], a conceptual design was made to investigate the feasibility. In particularly, the objective was to estimate the possible weight and power consumption of the system.

A double slotted guidance system was selected to deploy the flap as it could not be stowed vertically. The stack actuators were

positioned near the root of the blade to minimise their impact on the dynamics of the blade. Lever mechanisms with a long rod connect the actuators with their respective flap. The mechanism was constructed in such a way that the connecting rods are always under tension using a spring that also ensured that the flaps would be retracted in case of a rupture of any of the mechanical components.

It needs to be noted that the required transmission ratios for each of the flaps is achieved in 2 steps. The first step is included in the 1D actuation system model and the second step is modelled as 3D lever in the multi-body mechanism model. This solution enables the designer to try out different actuators and adjust the transmission ratio easily in the system model without the need to change the 3D mechanical model.

Subsequently, this mechanism is embedded 5 times in the blade model to drive the 5 required AGF. In Figure 6 the mechanical system is shown.

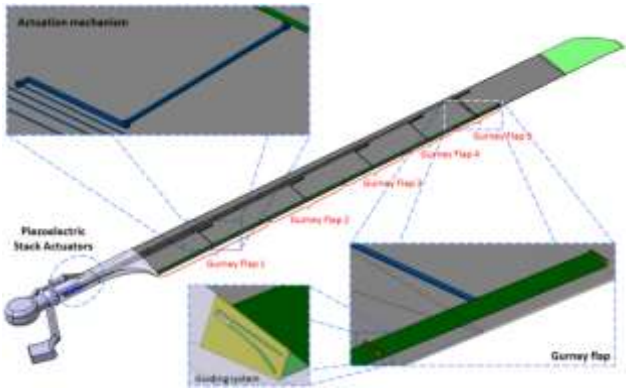

Fig 6. AGF actuation mechanism

The azimuth angle and blade rotation speed are measured in the Virtual.Lab Motion Blade model and sent to the controller modelled in Simulink through the system model, controlling the start of deployment and retraction of the different AGFs:

- Speed: AGF operation only starts when nominal rotation speed is reached.
- Azimuth angle: AGF is deployed and retracted according to selected operating condition

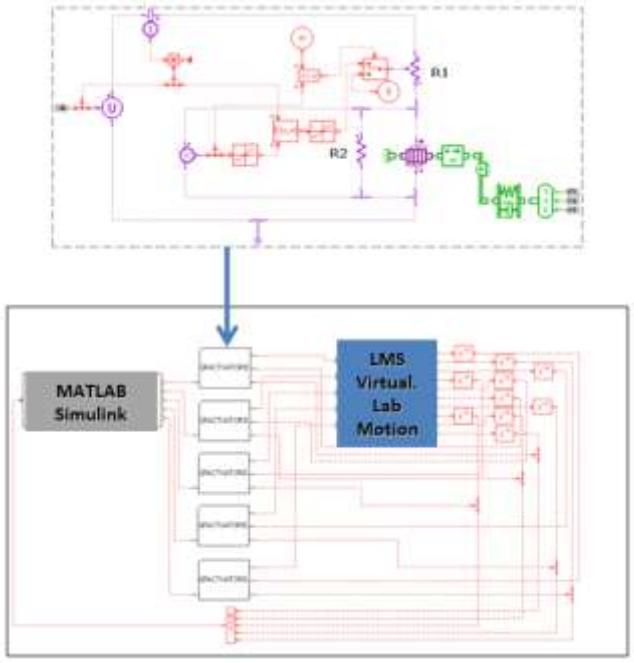

Fig 7. Actuation system model

The actuation system model is shown in Fig 7. In the lower part of the figure, the overall system model is shown. This includes on the left hand side the interface box with the controller model where it received the control voltage signals from for each of the 5 actuators. On the right hand side of the figure, the interface box with mechanism model is shown in blue where the actuators forces are send to and the displacements with velocities are received. In the middle, 5 identical boxes represent each actuator system. This actuation system is shown in more details at the upper part of the figure. This shows that the main components are a variable voltage source that is connected to a piezo-electric stack actuator by means of some variable resistors. The stack actuator is connected to a lever mechanism.

The controller model in Matlab/Simulink is shown in Fig 8. In the upper left corner, the operating condition selector can be seen. The output of the selector together with the blade position and velocity feedback from the mechanism is used as input for the control logic which is shown in the inset. In this case, a look-up table is used for the control logic. However, as mentioned earlier, also the nominal rotation speeds needs to be achieved before the flap operation starts. The output of the control logic

will be the voltage level that is sent to the actuation system.

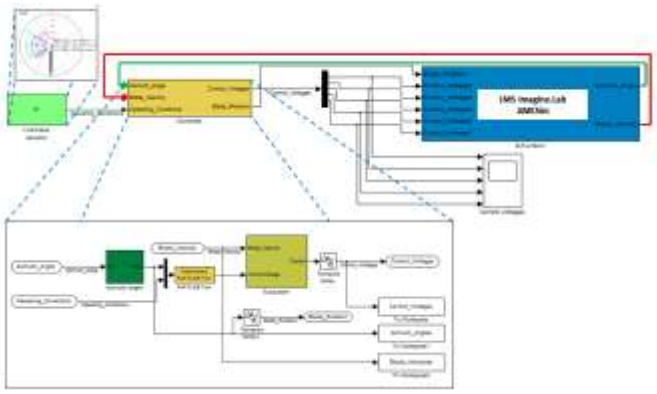

Fig 8. Controller model

As an extension of the single rotating blade, a full helicopter can also be modelled as shown in Fig 9. In this case the single rotating blade would be used in a LMS Virtual.Lab Motion as sub-mechanism. The same blade sub-mechanism can be introduced 4 times at 90deg into a full helicopter model to achieve the 4 blades of the helicopter with the corresponding integrated AGFs.

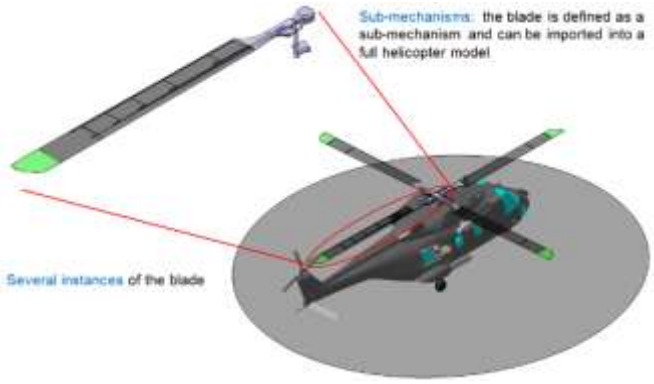

Fig 9. Integration of active blade in full helicopter model

7 Simulation Results

In this chapter some of the simulation results are presented, all considering the rotating blade with Operation Case III as the latter is considered the worst case because all 5 AGF are used. The first plot presents AGF deployment, control voltage, and azimuth angle for a full deployment-retraction cycle.

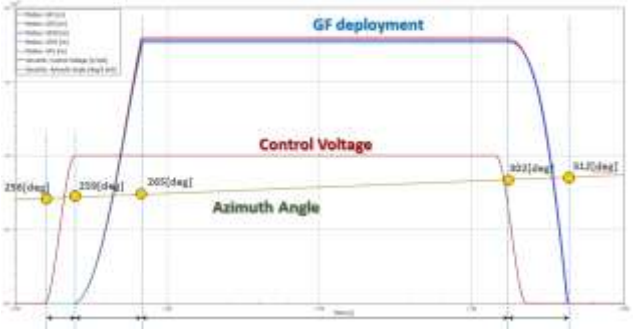

Fig 10. AGF deployment, Control voltage and Azimuth angle for the updated voltage control

As it can be seen in the plot, the AGFs deploy in 6 degrees and retract in 10 degrees as defined by the design requirement. Furthermore, the plot above presents also the control voltage signal, which as it can be noticed is increased from 0 to 1000V in 3 degrees. This control voltage signal is carefully chosen in order to meeting the deployment and retraction time requirements but also not to overload the system during the deployment or cause negative forces in the actuator during retraction. It can be noticed that the AGF deployment does not start immediately when increasing the voltage on the piezo electric actuators. The reason is that on one hand the force in the piezo actuators is gradually increasing as they are charged. The other hand, the AGFs will start to deploy only after the actuators first overcome the forces of the retractions system. Hence, the flaps deployment only starts when the actuator is fully charged.

The next plot in Fig 11, presents the electrical power requirements for deploying the first AGF. Two peaks can be observed, first when applying the voltage and second when decreasing the voltage on the piezo-electric actuator. These peaks can be reduced in the final design if applying the voltage over a wider azimuth angle range i.e. deploying and retracting the flaps more slowly. The sudden drop in the power curve after the AGF reaches the fully deployed state is due to the non-linear characteristics of the retraction spring.

Furthermore, the power requirements can be deducted from this plot by multiplying the

current with the voltage. As a result, power peaks will coincide with the current peaks.

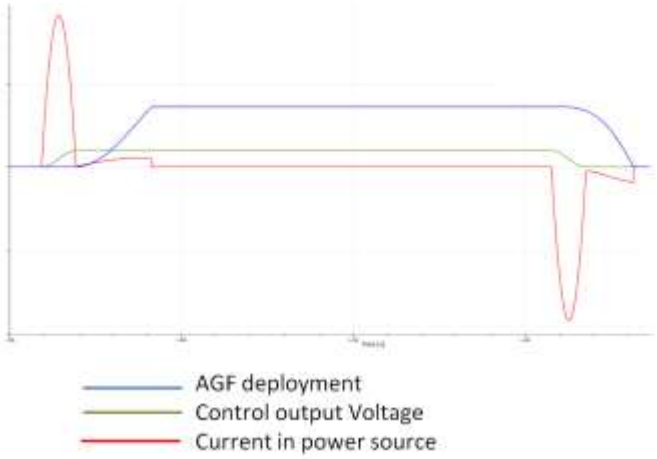

Fig 11. Electrical power requirements for deploying the first AGF

The final plot shows the forces in the 5 piezo actuators. Note that the maximum forces are achieved during the deployment but it is subsequently reduced when fully deployed because of the non-linear retraction spring. Further, it needs to be noted that all the actuation forces almost the same. This is because the length of the flaps was chosen to experience the same aerodynamic loads.

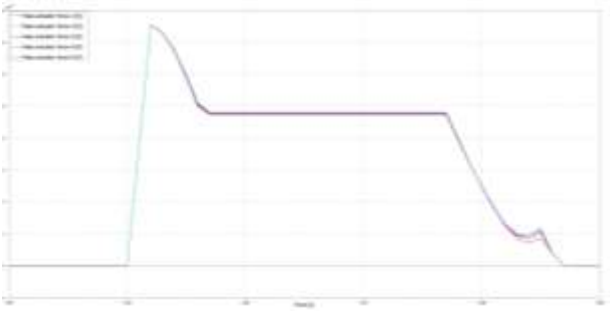

Fig. 12. Piezo-electric actuators forces corresponding to the updated voltage control

8 Conclusions

It is shown that an advanced co-simulation methodology can be used to design and analyse a complex integrated mechatronic system such as an AGF. In this case, three software tools, LMS Virtual.Lab Motion, LMS Imagine.Lab AMESim and Matlab/Simulink, where linked to simulate respectively the mechanism, actuation system and controller of an active Gurney flap system in a helicopter blade. It was concluded that the selection of the communication time interval between the tools is critical. Too large time steps will fail to capture the full dynamics of the system while too small time steps will lead to a large computational cost.

The presented results are for a first step of an iterative process to perform a complete design of AGF system in a helicopter blade. Therefore, the results are not of a final design. In particular, it can be observed that on the one hand the performance is possibly under-estimated because the maximum possible aerodynamic pressure at zero forward speed was used for all flaps and for all operating conditions. However, the performance of the AGF system will be overestimated because little mass and no friction of mechanical components are considered in the first results. The reason is the mass can only be determined when the required size of components are identified which will result in the loads in the system. As the latter is also impacted by the mass, it is clear that an iterative design process is required. However, making a final design was not the objective the reported activities as it was more a feasibility study. Furthermore, the subsequent design step will required more detailed simulation models. In particular, the friction and bending of the blade will be to be accounted for but this was also out of scope for these activities.

Nevertheless, from the presented initial results, it can be concluded that AGF system that is fully compliant with the original specifications will be difficult to achieve and will have a large weight penalty. It is anticipated that deploying and retracting the AGF over larger azimuth angles would reduce the system requirements. However, this will need to be supported with more aerodynamic studies. Furthermore, a smaller flap that can be stowed vertical would allow for a simpler and hence lighter mechanism which would compensate for the loss in aerodynamic efficiency. Also alternative actuation systems should still be investigated.

Acknowledgement

The research leading to these results has received funding from the European Community's Seventh Framework Programme (FP7/2007-2013) for the Clean Sky Joint Technology Initiative under grant agreement n° [CSJU-GAM-GRC-2008-001].

References

[1] AgustaWestland, *Clean Sky/Green Rotorcraft I.T.D. – Description of Work*, 2008.

[2] Busch M and Schweizer B, An explicit approach for controlling the macro-step size of co-simulation methods, *ENOC 2011*, Rome, Italy, 2011.

[3] Haug E. J., *Computer Aided Kinematics and Dynamics of Mechanical Systems*, Allyn and Bacon, 1989.

[4] Lemmens Y, Allain L and Olbrechts T. Development of design methodology for active Gurney flap system in helicopter rotor blade. *Proc Workshop on Aviation system Technology*, Hamburg, Germany, 2011.

[5] LMS International NV, *LMS Imagine.Lab AMESim Revision 10 Manual*, 2010

[6] LMS International NV, *LMS Virtual.Lab Revision 10 Manual*, 2010

[7] Maybury W and Carrus M, *Clean Sky/Green Rotorcraft I.T.D. – GRC1.1 Technology Review Document*, CS JU/ITD GRC/RP/1.1/31005, Agusta Westland, 2009.

[8] Maybury W, Carrus M and Dymott S, *Clean Sky/Green Rotorcraft I.T.D. – Specification for Advanced Rotor Configurations*, CS JU/ITD GRC/RP/1.1/31009, AgustaWestland, 2009.

[9] Paternoster A., *Assessment of mechanical constrains on a Gurney flap with CFD computation for IGOR project*, University of Twente, Engineering Technology, 2009.

[10] Paternoster A., de Jong P, Loendersloot R, de Boer A and Akkerman R, *Initial Technology Review, IGOR - Actuator and Control System for Green Rotorcraft I.T.D.*, University of Twente, Engineering Technology, 2009.

[11] Wang J.J., Li Y.C. and Choi K.-S., Gurney flap-Lift enhancement, mechanisms and applications, *Progress in Aerospace Sciences*, Vol. 44 (1), Pages 22-47, 2008.

[12] Yee K, Joo W and Lee D.-H, Aerodynamic performance analysis of a gurney flap for rotorcraft application, *Journal of Aircraft*, Vol. 44 (3), pp. 1003-1014, 2007.

Copyright Statement